



Michigan Technological University  
*Create the Future* Digital Commons @ Michigan Tech

---

Dissertations, Master's Theses and Master's  
Reports - Open

Dissertations, Master's Theses and Master's  
Reports

---

2011

## Local degradation of structural, mechanical, electrical and chemical properties of membrane electrode assembly in polymer electrolyte fuel cell

Nishith Parikh  
*Michigan Technological University*

Follow this and additional works at: <https://digitalcommons.mtu.edu/etds>

 Part of the [Mechanical Engineering Commons](#)

Copyright 2011 Nishith Parikh

---

### Recommended Citation

Parikh, Nishith, "Local degradation of structural, mechanical, electrical and chemical properties of membrane electrode assembly in polymer electrolyte fuel cell", Master's report, Michigan Technological University, 2011.

<https://doi.org/10.37099/mtu.dc.etds/558>

Follow this and additional works at: <https://digitalcommons.mtu.edu/etds>

 Part of the [Mechanical Engineering Commons](#)

Local Degradation of Structural, Mechanical, Electrical and  
Chemical properties of Membrane Electrode Assembly in Polymer  
Electrolyte Fuel Cell

By

Nishith Parikh

A REPORT

Submitted in partial fulfillment of the requirement for the degree of

MASTER OF SCIENCE

(Mechanical Engineering)

MICHIGAN TECHNOLOGICAL UNIVERSITY

2011

© 2011 Nishith N. Parikh

This report, “Local Degradation of Structural, Mechanical, Electrical and Chemical properties of Membrane Electrode Assembly in Polymer Electrolyte Fuel Cell”, is hereby approved in partial fulfillment of the requirements for the Degree of MASTER OF SCIENCE in Mechanical Engineering.

Mechanical Engineering-Engineering Mechanics

Signatures:

Report Advisor: Reza Shahbazian Yassar

Department Chair: William W. Predebon

## **Abstract**

Polymer electrolyte fuel cell (PEMFC) is promising source of clean power in many applications ranging from portable electronics to automotive and land-based power generation. However, widespread commercialization of PEMFC is primarily challenged by degradation. The mechanisms of fuel cell degradation are not well understood. Even though the numbers of installed units around the world continue to increase and dominate the pre-markets, the present lifetime requirements for fuel cells cannot be guarantee, creating the need for a more comprehensive knowledge of material's ageing mechanism. The objective of this project is to conduct experiments on membrane electrode assembly (MEA) components of PEMFC to study structural, mechanical, electrical and chemical changes during ageing and understanding failure/degradation mechanism.

The first part of this project was devoted to surface roughness analysis on catalyst layer (CL) and gas diffusion layer (GDL) using surface mapping microscopy. This study was motivated by the need to have a quantitative understanding of the GDL and CL surface morphology at the submicron level to predict interfacial contact resistance. Nanoindentation studies using atomic force microscope (AFM) were introduced to investigate the effect of degradation on mechanical properties of CL. The elastic modulus was decreased by 45 % in end of life (EOL) CL as compare to beginning of life (BOL) CL. In another set of experiment, conductive AFM (cAFM) was used to probe the local electric current in CL. The conductivity drops by 62 % in EOL CL.

The future task will include characterization of MEA degradation using Raman and Fourier transform infrared (FTIR) spectroscopy. Raman spectroscopy will help to detect degree of structural disorder in CL during degradation. FTIR will help to study the effect of CO in CL. XRD will be used to determine Pt particle size and its crystallinity. In-situ conductive AFM studies using electrochemical cell on CL to correlate its structure with oxygen reduction reaction (ORR) reactivity

## **1. Introduction**

The polymer electrolyte membrane fuel cell (PEMFC) is widely regarded as a key technology in building a hydrogen fuel-based renewable energy economy. Fuel cells convert chemical energy to electricity, working like a battery with continuous fuel and oxidant feeds. In an economy running on renewable energy sources these devices could be used for portable power or load-leveling, generating electricity in mobile or stationary applications at times of high demand and low supply from hydrogen that is created and stored when electricity is more available. PEM fuel cells are seeing early application in extended-life power supplies for laptop computers and cellular phones as well as automobiles. The MEA structure comprising of gas-diffusion layer/anode catalyst/electrolyte/cathode catalyst/gas-diffusion layer composite is shown in Figure 1.

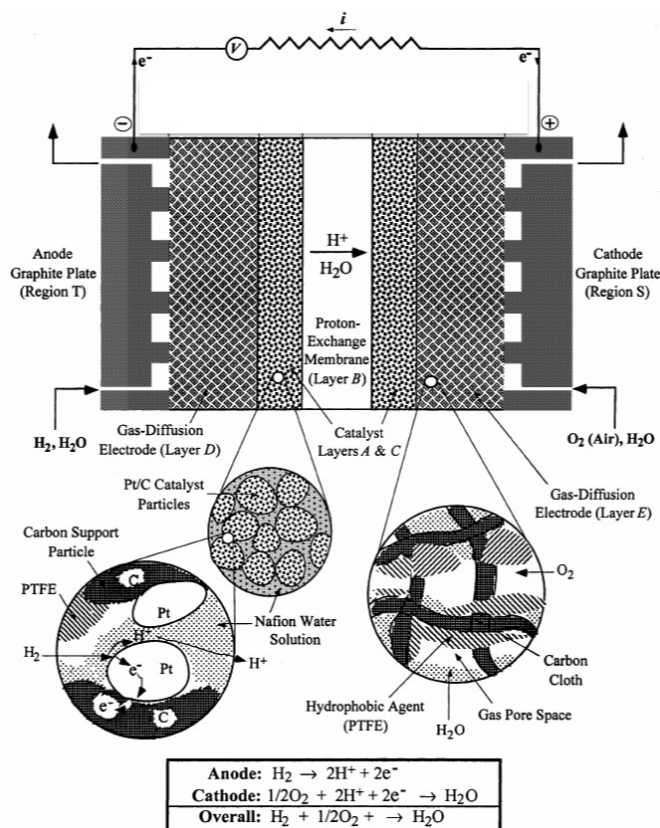


Figure 1. A schematic representation of the PEM fuel cell cross-section consisting of GDL (layers D and E), CL (layers A and C), and the PEM (layer B).<sup>i</sup>

$\text{H}_2$  is split into protons and electrons at the anode electrocatalyst. Protons find their way to the cathode through the PEM, while the electrons arrive at the cathode via the external circuit after performing useful work. Here, aided by electrode potential, the protons and electrons recombine with  $\text{O}_2$  at the catalyst surface to form water. The MEA is sandwiched between two graphite plate current collectors with machined microchannels<sup>ii</sup> for gas distribution.

The CL (layer A and C) is 5–20 $\mu\text{m}$  in thickness and contains Pt particle, roughly 2–4nm in diameter, supported on the surface of largely non-porous carbon black particles, around 30nm in diameter, at a Pt/C loading of about 20–45 wt.% and  $\leq 0.4 \text{ mgPt}/\text{cm}^2$  of MEA area.<sup>iii</sup> The GDL (layers D and E) serves as the electron collector and a permeator for reactant gases as well as for liquid water. The carbon cloth is treated with 40–70 wt.% poly-tetrafluoroethylene (PTFE, e.g., Teflon<sup>®</sup>) mixed with 10–20nm carbon particles followed by sintering to melt the PTFE and coat the carbon fibers and rendering it quite hydrophobic. The porosity of the GDL is 70–80%.<sup>iv</sup> A polymer electrolyte membrane (PEM), 50–175 $\mu\text{m}$  thick, is hot-pressed at a temperature slightly above its glass transition temperature between the two electrodes such that the CL are on either side of the membrane.<sup>v</sup>

Due to stability and water management issues, the operating temperature of the PEMFC is limited to around 70°. At this temperature, the low exchange current density of the oxygen reduction reaction necessitates a large amount of precious metal catalyst. The key goals of fuel cell catalyst research are to increase the activity and utilization

levels of the catalyst while reducing the catalyst loading. These dual goals provide double rewards by simultaneously reducing costs and improving performance.

An ideal CL should have: 1) a large interface between gas phases and/or polymer electrode and catalyst, 2) highly efficient proton transport, 3) high transportation capacity for oxygen and easy by-product removal (i.e., condensed or gaseous water), 4) high electronic conductivity, 5) excellent chemical resistance and good mechanical properties to maintain an effective porous structure during fuel cell operation, and 6) high tolerance to contamination. A schematic of Pt/C structure is shown in Figure 2.

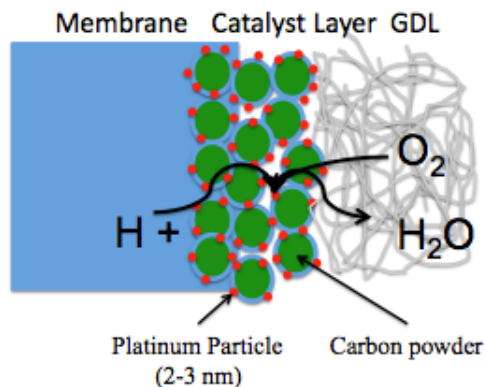


Figure 2. Schematic of Pt/C catalyst structure

While platinum provides the catalytic activity, the carbon provides the electrical conductivity necessary to harvest or deliver electrons to the active sites. In a standard PEMFC catalyst structure, the Pt/C powder is mixed with small quantities of the Nafon electrolyte. (This is usually accomplished via liquid phase ink, where the Pt/C is dispersed in a Nafon solution.) The ink is applied to the electrodes or membrane of the fuel cell and allowed to dry, leaving behind a porous, 3-dimensional mixture of Nafon, platinum, and carbon. This mixture serves to simultaneously increase the conduction path for both ions and electrons as to maximize the total amount “three-phase zone”, where the electrode, electrolyte, and gas phases meet. The three-phase zone, or triple phase boundary area is where the fuel cell electrochemical reactions take place. The thickness of the CL is between 10-50  $\mu m$ . While a thin layer is preferred for better gas diffusion and catalyst utilization, a thick layer incorporates higher catalyst loading and presents more three-phase zones. Thus, CL optimization requires a delicate balance between mass transport and catalytic activity.

Reliability and durability are the most important considerations in PEMFCs. The durability of catalysts has become a major concern in fuel cell development. Under fuel cell operating conditions, the cathode CL can degrade through platinum sintering and dissolution, especially in conditions of load-cycling and high electrode potentials. Carbon support corrosion is another challenge at high electrode potentials and can worsen under load cycling and high temperature operation. Although significant attention has been focused upon fundamentally understanding catalyst degradation and the development of novel catalysts and structures, we are not yet close to making durable electrodes at low cost for the commercializing of fuel cells.

## 2. Literature Review

Cathode catalyst degradation is mainly caused by loss in the electrochemical active surface area (ECSA) of Pt or its alloys. Loss of surface area (for Pt or its alloys) in the fuel cell is believed to occur by combination of the following four processes<sup>vi,vii,viii,ix,x</sup>:

1) formation of larger particles via Pt dissolution from smaller particles (Ostwald ripening); 2) coalescence of Pt nanoparticles by thermal motion (sintering) or loss of the carbon support due to carbon corrosion; 3) Pt migration into the catalyst electrolyte or membranes, and 4) Pt trapped in the CL ionomer during electrode fabrication. Carbon corrosion could lead to damage of the porous structure of the CL, resulting in increased mass transport loss.

As demonstrated by many researchers, agglomeration and particle growth of the nanostructure of Pt is the most dominant mechanism for catalyst degradation in PEM fuel cells.<sup>xi,xii</sup> Nano-sized structural elements are able to show size-dependant properties different from bulk elements.<sup>xiii</sup> Nano-particles have the inherent tendency to agglomerate into bigger particles to reduce the high surface energy. Ferreira et al.<sup>vii</sup> analyzed degraded MEAs after 2000 h of operation under open-circuit voltage (OCV) in a H<sub>2</sub>/air cell and explained that small Pt particles dissolve in the ionomer phase and redeposit on larger particles that are separated from each other by a few nanometers, forming a well-dispersed catalyst, called “Ostwald ripening”. Virkar and Zhou<sup>xiv</sup> explained that Ostwald ripening, involving coupled transport of electrically charged species, is the main reason for particle growth in Pt/C catalysts, where the Pt is transported through the liquid and/or through the ionomer and the electrons through the carbon support. Other groups<sup>xv,xvi,xvii</sup> and believed that two other mechanisms are predominately responsible for degradation during the potential cycling process: (1) Pt particles detaching from the support and dissolving into the electrolyte without re-deposition, and/or (2) a combination of Pt particle coalescence and Pt solution/re-precipitation within the solid ionomer. In addition, the agglomeration of Pt can also be affected by many other operating conditions such as temperature and relative humidity.

Pt loss during operation is another major source of CL degradation. This can be caused by many factors such as Pt dissolution and washout. Luo et al.<sup>xviii</sup> conducted an experiment involving a 10-cell stack operating for 200 h under ambient humidity, ambient pressure and 60 °C. Pt content in the Pt/C CL was determined by atomic adsorption spectroscopy. The results showed that the Pt content was only 13.5% compared to the original value of 20%, which proved that there are serious Pt losses during the aging process. By weighing and using inductively coupled plasma combined with mass spectrometer (ICP-MS), respectively, Mitsushima et al.<sup>xix</sup> and Ball et al.<sup>xx</sup> also measured Pt loss from the Pt/C catalyst in acidic electrolyte systems after potential cycling.

Pt migration within MEA has been observed to have the same effect as Pt loss. Many groups<sup>xxi,xxii,xxiii</sup> have reported the presence of Pt particles inside the PEM as well as enrichment of Pt in the CL/PEM interface under different conditions. Pt catalyst particles were observed within the PEM and near the CL/PEM interface after degradation.<sup>xxiv</sup> These Pt particles originate from the dissolved Pt species, which diffuse in the ionomer phase and subsequently precipitate in the ionomer phase of the electrode or in the membrane. Ferreira et al.<sup>vii</sup> and More et al.<sup>xii</sup> observed Pt enrichment at the cathode/membrane interface, while Xie et al. [14] and Guilminot et al.<sup>xxiii</sup> observed Pt

enrichment at the anode/membrane interface. The main reason for the diversity of results is that Pt migration and redistribution is a complex process affected by many factors such as potential, operating time, potential cycle numbers, cell operating conditions, gas permeability of the membrane, and other component conditions.

Under prolonged operation at high temperatures, high water content, low pH, high oxygen concentration, existence of the Pt catalyst and/or high potential, carbon support is prone to degrade both physically and chemically, which is called carbon oxidation (or carbon corrosion). Carbon oxidation weakens the attachment of Pt particles to the carbon surface, and eventually leads to structural collapse and the detachment of Pt particles from the carbon support, resulting in declines of the catalyst active surface area and fuel cell performance.

Many different investigative tools, including electrochemical and physical/chemical methods, have become available that investigate CL degradation. Structural characterization methods provide valuable information on morphology, surface or cross section of the CL and size distribution of the catalyst particles. Table 1 summarizes the structural analysis tools in catalyst degradation research.

Table 1. Summary of structural analysis methods for MEA studies

<b>Technologies</b>	<b>Characteristics</b>	<b>Information</b>	<b>Reference</b>
TEM (transmission electron microscopy)	Morphology or Pt distribution analysis	Topography investigation and particle size distribution	ix·xii·xvii·xxiv,xxv,xxvi,xxvii
SEM (scanning electron microscopy), FESEM, SEM-EDS		Topography investigation and elemental distribution analysis of a cross section of an MEA or CL	ix·xi·xii·xviii·xxiii,xxviii
AFM (atomic force microscopy)		Morphology of the surface of the carbon substrate	xxviii,xxix
3-D X-ray CT (3D X-ray computer tomography)		Investigate changes in the internal morphology, Pt distribution and carbon content, etc.	xxx,xxxi

There are spatial and temporal variations in water content due to non-uniform electrochemical reactions caused by phenomena such as uneven feed distribution in gas distribution channels, localized hot spots and catalyst poisoning. These variations across MEA cause differential swelling, thereby creating internal stresses that result in deformation and failure of MEA. Table 2 summarizes the investigation tool use for mechanical and electrical characterization of MEA degradation in PEM fuel cell.



Table 2. Summary of mechanical/electrical studies on MEA

Technologies	Characteristics	Information	Reference
Nanoindentation	Mechanical properties and fracture characteristics	Elastic modulus and Hardness	lxvi·lxvii
MTS testing machine	Tensile and creep analysis	Stress vs strain curve, surface cracks	xxxii
cAFM (conductive AFM)	Proton conductivity	Ionic network distribution	xxxiii,xxxiv

In addition to structural and mechanical properties, more information about changes in the catalyst surface structure can be obtained from chemical measurements Table 3 summarizes the chemical investigation methods to find elemental content and distribution and atomic structure of the local particles inside the CL.

Table 3. Summary of chemical analysis studies on MEA

Technologies	Characteristics	Information	Reference
AAS (atomic adsorption spectroscopy)	Elemental content analysis	Investigate the Pt content in the Pt/C catalyst	xviii
LRS (laser Raman spectroscopy)	Atomic structure analysis	Detect the degree of structural disorder of carbon	xxxv
XPS (X-ray photoelectron spectroscopy)		Surface oxygen content or electronic structure change of other surface elements	xxiii,xxxvi,xxxvii
XRD (X-ray diffraction)		Pt particle average sizes and crystallinity of alloy materials analysis	xi·xvii·xxxvi,xxxviii

### 3. Technical Plan

#### 4.1 Completed Tasks

**Task 1.** Surface roughness measurements of GDL and CL.

**Task 2.** Local mechanical properties of BOL and EOL CL.

**Task 3.** Local electrical properties in EOL CL

#### Task 1: Surface Roughness Properties of GDL and CL

Surface roughness and topology of fuel cell components are influential on both thermal and electrical contact resistance losses, and this influence has been studied extensively by analyzing the bipolar plate (BPP) and GDL interface.<sup>xxxix,xl,xli,xlii,xliii,xliv</sup> Surface treatments, which cause modifications in BPP surface characteristics, were shown to cause substantial changes in BPP|GDL interfacial contact resistance, and several modeling studies were conducted to predict the BPP|GDL interfacial contact resistance<sup>xxxix,xl</sup> by taking the surface profiles of BPP and GDL into consideration.<sup>xlii-xliii</sup> However, little has been done to investigate the GDL|CL interfacial contact resistance, except a few experimental studies that were limited to measuring the bulk contact resistance rather than focusing on surface morphology of these layer.<sup>xliv,xlvi</sup> Due to rough nature of GDL and CL surfaces, the contact between these layers will be imperfect under compression.

This will result into formation of interfacial gaps with uneven compression pressure between GDL and CL surface and consequently reduction in contact area as shown in Figure 3.

Figure 3. Schematic of GDL|CL interfacial contact

The contact resistance is predicted from the following analytical model which is derive from hertzian theory of contact as shown in equation 1.

$$R = \frac{4}{\rho_1 + \rho_2} D_{sum} R \sigma_s F\left(\frac{d}{\sigma_s}\right) \quad (1)$$

where  $\rho$  is the resistivity of material,  $R$  is the contact radius,  $d$  is the height of the single summit,  $D_{sum}$  is the density of the surface and  $\sigma_s$  is the sum of height variables.

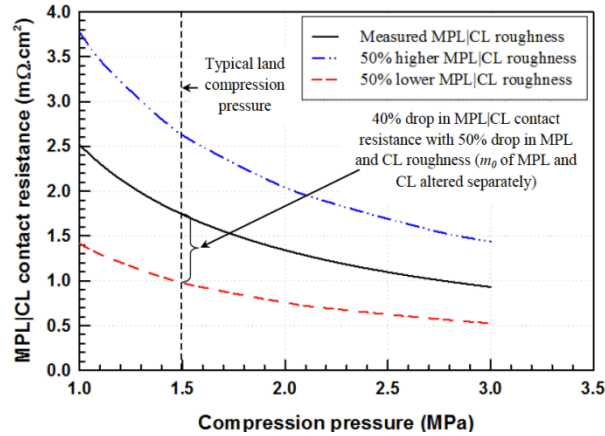


Figure 4. Predicted MPL|CL contact resistance versus compression pressure for different degrees of MPL and CL roughness.

Figure 4 shows the variation of the predicted MPL|CL contact resistance as a function of the applied compression pressure for different degrees of uncompressed roughness of the mating surface profiles. The optimum assembly pressure occurred at between 0.5 MPa and 1 MPa pressure values; a condition which provided a highly efficient operating condition of the fuel cell.<sup>xlvi</sup> It can be seen from Figure 4 that lowering the roughness of the MPL and CL surfaces by 50% results in nearly a 40% drop in the MPL|CL interfacial resistance. This significant drop in the contact resistance can be attributed to the fact that as the roughness of the mating surfaces is decreased, the number of contact points increases, which in turn, facilitates the electron flow across the MPL|CL interface.

There exists a gap in the literature regarding how the GDL and CL surface morphologies, and the interfacial voids that occur between them, affect the various fuel cell polarization losses. This can be attributed to the experimental limitations involved in the three-dimensional characterization of the porous and highly irregular surfaces of the GDL and CL. In the reported studies, optical microscope, SEM and AFM have been commonly employed to characterize the GDL and CL surface topography.<sup>xlvi,xlviii,xlix</sup> When compared, optical microscope measurements provide a relatively poor description of the GDL and CL surfaces due to relatively smaller depth of focus and limited resolution capabilities. Even though SEM imaging can provide a good overall view of the surfaces in two dimensions, it yields limited quantitative information regarding the height values of surface perturbations in the vertical direction. Moreover, direct acquisition of quantitative roughness values from two-dimensional SEM images is not possible. AFM can give three-dimensional data and quantitative roughness information compared to SEM. However, due to the highly rough nature of GDL and CL surfaces, the scanning area in AFM is limited to only few hundred square micrometers and the measurement speed is very small. Surface of the BOL GDL and CL were investigated using surface mapping microscope in order to evaluate surface roughness.

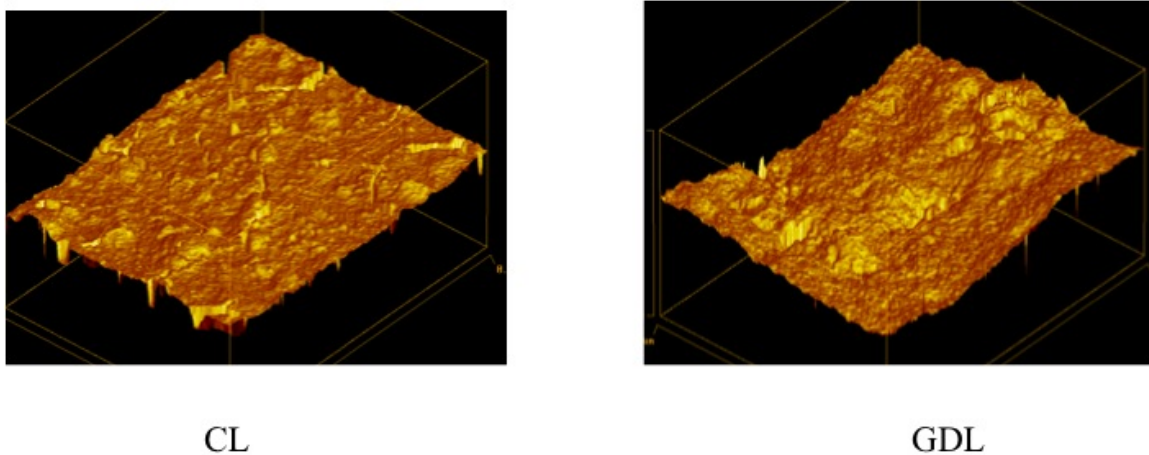


Figure 5. Surface roughness measurements of CL and GDL from surface mapping microscope

ADE Phase Shift MicroXAM surface mapping microscope was used to measure surface roughness of GDL and CL. This is a non-contact profiler having a repeatability of

0.1 nm and vertical resolution of 4nm. The scan size was 900 x 800  $\mu\text{m}$ . Since the GDL and CL possess low reflectivity and have light dispersive characteristics, the surface was sputtered with a thin layer of gold. The average roughness of GDL and CL was found to be 4.1  $\mu\text{m}$  and 3.2  $\mu\text{m}$  respectively which agrees with the Hizir et al.<sup>1</sup> who obtained the surface roughness of GDL and CL as 5.35  $\mu\text{m}$  and 2.19  $\mu\text{m}$  from optical profilometer (Figure 5). It's a good technique that provides a noncontact, 3-D method of measuring surface roughness.

## **Task 2: Local Mechanical Properties of BOL and EOL CL**

Microstructure changes in CLs may occur in several ways, such as chemical degradation of the ionic conducting parts or mechanical failure.<sup>ix,li,lii</sup> Although chemical degradation is a key factor in microstructure changes, it has been suggested that mechanical damage also plays an important role.<sup>liii,liiv</sup> For example, debonding between the electrolyte and the carbon-catalyst agglomerate directly results in a loss of carbon-supported catalyst clusters, while the breaking of the electrolyte network contributes to the dissolution of the proton-conducting network. Karlsson et al.<sup>liv,lv</sup> used a model to simulate the mechanical analysis of the MEA scale. As a result of the start-up and shutdown of the fuel cells, humidity and temperature fluctuate and influence the mechanical behavior of different MEA components. They found that critical residual stresses accumulate and lead to mechanical fatigue in the membranes after a hydrothermal cycle. However, the mechanism of microstructure changes in CL is still unclear. Mechanical damage in the CL can appear as flaws or mud-cracks<sup>lii</sup>, delamination between the carbon-catalyst agglomerate and the electrolyte<sup>lvi</sup> or corrosion of carbon. In this study, the mechanical properties of catalyst at micro scale are done by nanoindentation AFM. Nanoindentation is commonly used for measuring nano- or microscale mechanical properties of thin films. However its application is not only limited to films. This technique has become ubiquitous in characterizing the mechanical properties of materials whose properties are size or small volume dependent. Recently, nanoindentation has been applied to characterize the mechanical properties of nanowires<sup>lvii,lviii</sup>, CNTs<sup>lix</sup>, amorphous carbon films<sup>lx</sup>, nanobelts<sup>lxi</sup>, biological tissues<sup>lxii,lxiii</sup> and nanocomposites.<sup>lxiv</sup> The obtained values of load and displacement as a function of depth or time are used to calculate the hardness and elastic modulus. It is also possible to establish a relation between contact stiffness and displacement and from this, material under investigation can be classified as a graded or uniform one. Sensing its capability to characterize the individual constituents within the heterogeneous sample, it can well be adopted in obtaining the mechanical parameters of CL. Indentation of catalyst surface by a sharp indenter provides quantitative information related to contact stiffness that can be referred to an amount of resistance that the material can withstand from an external force in the normal direction. Commercial nanoindenters do not offer a wide range of loads necessary for soft materials. Another advantage of AFM over conventional indentation is that it measures the contact area and depth from the imaging data directly with the same tip used to obtain the force–displacement curve. The hardness and Young's modulus can be directly obtained from the imaging data.

A nanoindenter mounted on AFM was used for nanoindentation tests. A Berkovich tip was used for indentation and imaging experiments. A small tip is pressed

into a sample with a known load (force) and retracted sequentially, which generates a force–displacement curve. With the force–displacement curve, the elastic modulus can be obtained by applying the Hertz model.<sup>lxv</sup> Three indentations were made on each CL sample. Calibration was done for deflection sensitivity, radius tip, and spring constant in order to quantify the forces as well as the mechanical properties. Figure 6 shows a typical indentation load versus displacement curve, including both loading and unloading, on BOL and EOL CL. Blue line indicates the tip to surface approach while red line indicates the retract motion.

As there is no adhesion between the sample and tip, Hertz model [42] is used to calculate elastic modulus of CLs from the force –separation curves using the equation below:

$$F = \frac{4E\sqrt{R}}{3(1-\nu^2)}\delta^{3/2} \quad (1)$$

Where  $F$ ,  $E$ ,  $R$ ,  $\nu$  and  $\delta$  are peak force, elastic modulus, tip radius, poison ratio, and deflection sensitivity.

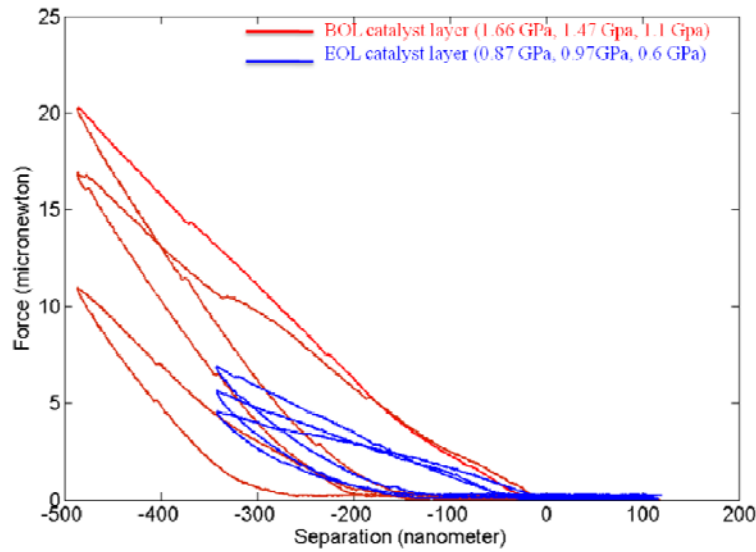


Figure 6. Force - separation curves of BOL and EOL CL. Red lines indicate BOL CL and the blue lines is EOL CL.

The Hertz model was fitted to 75% of approach curve to minimize the effect of inelastic deformation. The calculations show that the elastic modulus of BOL CL is 1.41 GPa while this value for the EOL CL is 0.81 GPa. This is in agreement with the elastic modulus of CL reported by Pooresh et al<sup>lxvi</sup>, which is 1.68 GPa (using nanoindentation). The elastic modulus decreased by 57 % in EOL CL. It is believed fuel cell working conditions such as operating temperature, external compressive loads and temperature are primary factors in decrease of elastic modulus in EOL CL. Another article by Pooresh et al<sup>lxvii</sup> have shows through numerically simulation the effect of nanoporosity on mechanical strength by analyzing the CL structure based on the elastic modulus. They said CLs have the elastoplastic ionomer matrix and anisotropic nanoporosity, which are

responsible for the localized plastic densification on indentation. There is a significant structural change in EOL CL. A structural change caused by the loss of carbon particles could result in deterioration of the integrity of CL.

### Task 3: Local Electrical Properties in EOL CL

cAFM is a powerful current sensing technique for characterizing conductivity variation in samples. This technique is useful to obtain current image and electrical conductivity of the catalyst surface. In this method, a conducting cantilever scans the sample surface and by applying a bias voltage between the cantilever and the sample the local conductivity can be monitored. It detects the resulting current flow, which can be as low as a few pA. A bias voltage between the sample and conducting cantilever was 500mV with current sensitivity of 100 nA/V during all imaging experiments. The sample was silver painted on edge of the sample to make it conductive.

The cAFM technique was used to obtain the current images of BOL and EOL CL (Figure 7a and b). The white area in current image shows high current range between 1-1.2  $\mu$ A. The red, green and yellow areas have medium current range between 0.2 -1  $\mu$ A. The black area shows very low current usually in 50-100 nA. EOL CL appears to be less conductive than the BOL sample. The percentage of the conductive area (Figure 7c) shows that in BOL CL, 51 % of area has current of 1.2  $\mu$ A or higher while in EOL CL it reduced to 19%. The conductivity area drops by 62% in EOL CL.

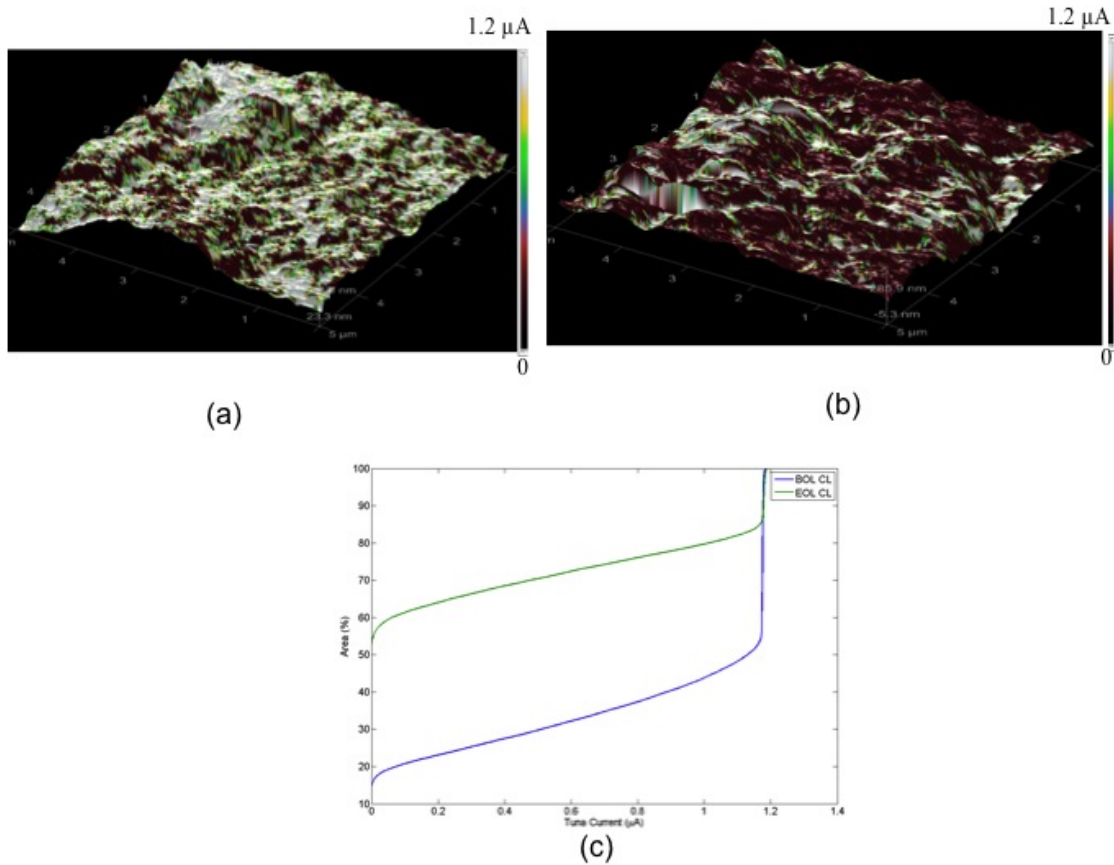


Figure 7. Current images of (a) BOL CL (b) EOL CL. The scan size is 5  $\mu$ m. (c) Percentage of conductive area showing current distribution of BOL and CL

The carbon support is thermodynamically unstable under fuel cell operating conditions hence it slowly (under normal conditions) oxidizes to carbon dioxide.<sup>lxviii</sup> Carbon oxidation gradually reduces carbon mass and degrades the electrical contacts between individual carbon particles. This carbon corrosion results in lower electrical conductivity<sup>lxix</sup> of the carbon phase in the EOL CL. Lower electrical conductivities of carbon could cause severe cell performance loss.

## 4. Future Tasks

### Task 4: Chemical Characterization of Degraded MEA

Raman spectroscopy is frequently used in the fuel cell research for the ex-situ characterization of fuel cell components mainly polymer electrolyte membrane.<sup>lxx</sup> This experiment will be done to detect the degree of structural disorder of carbon in CL during degradation. Cheng et al<sup>lxxi</sup> has characterized Pt/Ru/C catalyst samples obtained from fresh and tested MEAs with Raman spectroscopy. In Figure 8a they showed two characteristic Raman bands associated with amorphous carbon appeared near 1334 and 1597  $\text{cm}^{-1}$ . They observed values of intensity values were reduced after cell test, which indicate low degree of graphitization and amorphous carbon.

To help identify the cause of Pt surface area loss, X-ray diffraction (XRD) will be use to measure the particle size to determine the degree of catalyst sintering. Cheng et al<sup>lxxi</sup> has measured particle size of catalyst using XRD and was found to increase with cell operating time. The peaks observed near  $2\theta$  angles of 40 and 46° in Figure 8b corresponded to Pt (111) and Pt (200). The strongest peak, Pt (111), tended to become narrower in the cathode diffraction spectra after different lifetime tests. The average particle size of the catalysts can be calculated from XRD using a Scherrer equation by a full-width at half-maxima (fFWHM) which is determined by fitting the Pt (111) peak with a Lorentzian function as shown in equation 2.<sup>lxxii</sup>

$$t = \frac{K \cdot \lambda}{B \cdot \cos \theta_B} \quad (2)$$

Where  $t$  is thickness of crystallite,  $K$  is constant dependent on crystallite shape,  $\lambda$  is x-ray wavelength,  $B$  is FWHM and  $\theta_B$  is Bragg angle. The crystal size of Pt catalyst increases from 3.2 to 5.8 nm. We will correlate this growth of particle size to conductive area obtained from cAFM.

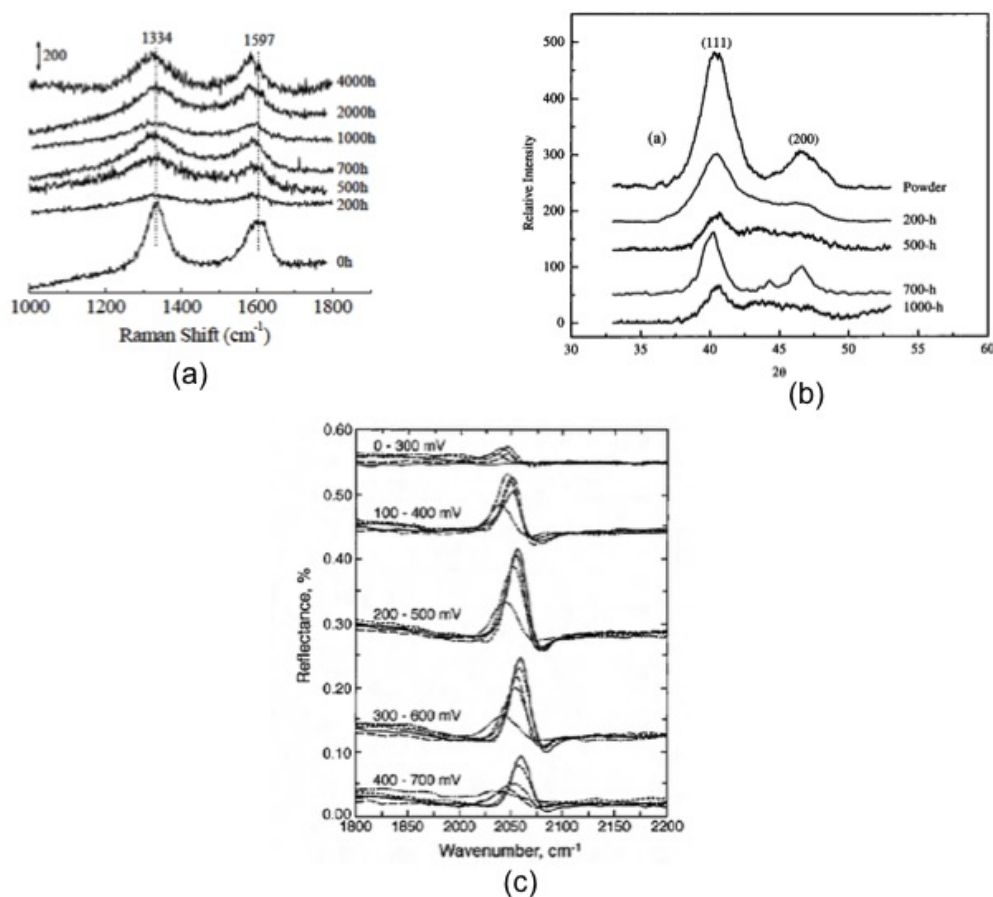


Figure 8. (a) Typical Raman spectra of PtRu/C catalysts from MEAs before and after different periods of cell tests (b) XRD patterns of cathode catalyst after different lifetime tests (c) Collection of CO FTIR spectra for five different sized carbon-supported Pt nanoparticles.

Another likely cause of severe degradation of the CL in PEMFC is contamination from the fuel and the air such as CH<sub>4</sub>, CO, CO<sub>2</sub>, H<sub>2</sub>S, NH<sub>3</sub>, NO, NO<sub>2</sub>, and SO<sub>2</sub>. FTIR has been used by many researchers for characterization of low-temperature fuel cells and has been widely used to investigate the mechanisms of adsorption and poisoning of catalysts, especially for DMFCs.<sup>lxxiii, lxxiv, lxxv</sup> FTIR is a very important tool to study the adsorption, migration, and poisoning mechanisms of carbon monoxide and other intermediates, and this research is of significant benefit in the exploration and development of CO-tolerant catalysts for PEMFCs. Rice et al.<sup>lxxvi</sup> has used *in situ* electrochemical FTIR to study a carbon-supported platinum + ruthenium catalyst. Figure 8c shows a collection of FTIR spectra of CO adsorbed on different size carbon-supported Pt nanoparticles, recorded at five potential step ranges. These results show that the CO peak position is dependent on the size of the carbon-supported Pt nanoparticles. In particular, CO adsorbed onto the smallest particles (2.0 nm in diameter) has the lowest vibrational frequency. Along with CO, FTIR can also help to study other contamination in CL.

Raman spectroscopy has been used to detect the metal oxide formation in CL. There are couple of articles<sup>lxxvii, lxxviii</sup> which has reported formation of ruthenium oxide in



anode CL. Though formation of Pt oxide has been reported previously and suggested to be responsible for failed MEA<sup>lvi</sup> but Raman spectroscopy has not been done to validate it. Most of FTIR spectroscopy work on carbon poisoning has been reported for anode CL. There is a lack of data for carbon poisoning in cathode CL.

### **Task 5: Determining the Effect of Carbon Loading**

The microporous layer (MPL) thickness is primarily controlled by the applied carbon loading. It is generally accepted that a thin MPL improves gas transport and facilitates the removal of water, but it has high electronic resistance and does not give a non-permeable support for coating with the CL while a thick MPL hampers gas accessibility because of the lengthened path through the MPL and also has poor gas diffusivity. Hence, an intermediate carbon loading may be beneficial.<sup>lxxvii lxxviii</sup> Also, Song et al.<sup>lxxix</sup> showed that optimal carbon loading of the MPL yielded the maximum active area for the catalyst in the CL. There are hardly any articles on the effect of carbon loading in CL. High surface area carbon (HSAC) gives appropriate platinum particles dispersion over the substrate but can lower the fuel cell performance.<sup>lxxx</sup> This is because HSAC are constituted of small primary carbon particles covalently linked as aggregates which agglomerate by soft bonds (Van der Waals) yielding small pores and these small pores can hinder transport mechanisms to the Pt particles. All the above experiments were done on low surface area carbon (LSAC) CL. We are planning to run similar experiment on medium surface area carbon (MSAC) and HSAC to study the effect of carbon loading on CL.

### **Task 6: In Situ cAFM Studies**

In Task 4, we have shown how conductive AFM can be used to detect conductivity of CL. Here we proposed a method using in-situ cAFM to correlate the structure and the relative reactivity at catalyst concerning ORR.<sup>lxxxi</sup> The investigation will be done under humid condition or in-situ in an electrochemical cell under potentiostatic control of tip and sample. Figure 9a shows the schematic of experimental set up. Current flow is observed when the negative voltage applied to the lower electrode (in contact with the sample holder) against the STM tip exceeds about 100 mV. Due to the closed current circuit and the fixed bias voltage between upper electrode and tip, normal electrochemical current image can be obtained (Figure 9b).

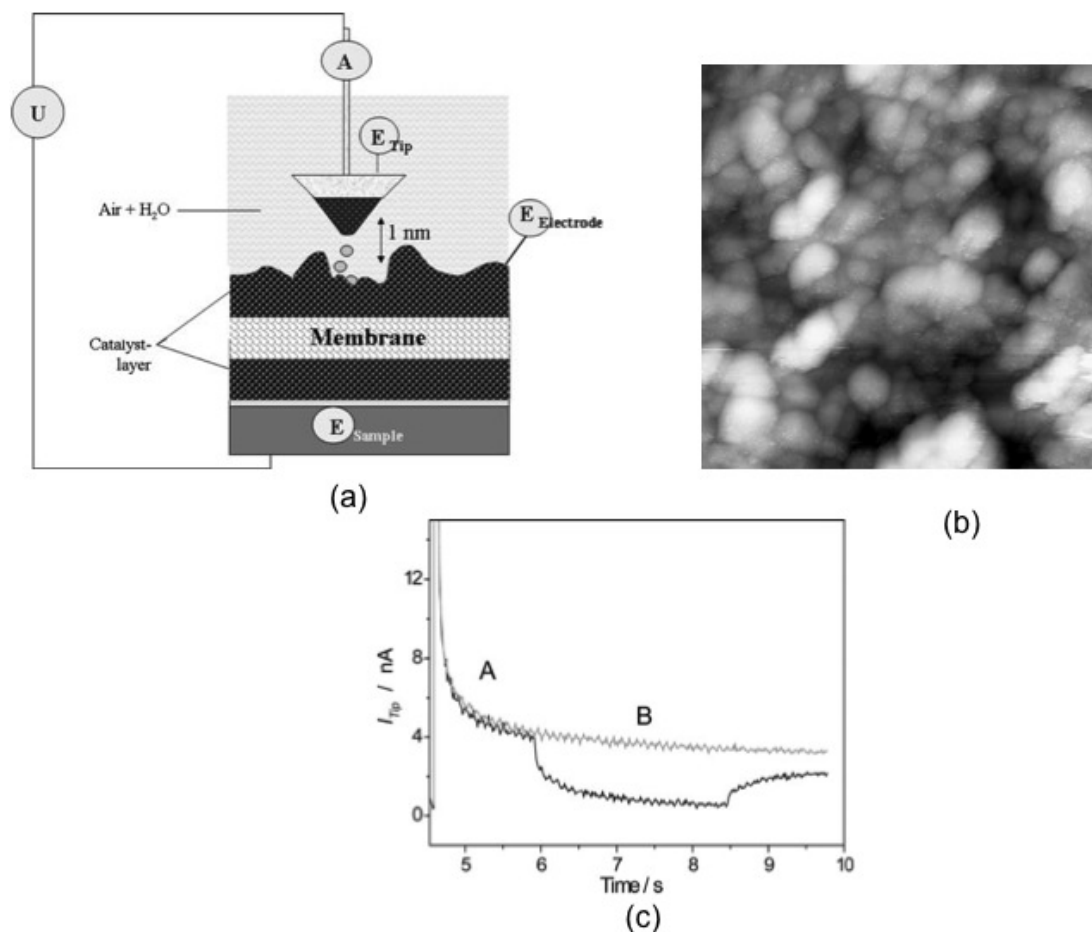


Figure 9. (a) In-situ method for imaging of CL using electrochemical cell. (b) Current image of CL. Scan size 100 x 100 nm. (c) Current through the STM tip after oxygen evolution at the tip without oxygen reduction (upper curve) and with oxygen reduction (lower curve) at a Pt foil. Time interval “A”: reduction of oxygen at the tip, time interval “B”: reduction of oxygen at the tip and at the sample (Pt foil).

The elliptical carbon particles are clearly visible and have a diameter of about 10 nm. On the surface of the carbon the individual platinum catalyst particles are visible having diameter of about 1–2 nm. The AFM tip is used as an electrochemical sensor for oxygen and the current through the AFM tip during oxygen reduction can be measured. Figure 9c shows the plot of current through the AFM tip after oxygen generation at the tip and reduction of the resulting oxide layer. A Pt foil is used as the sample. At a time of 4.5 s on the time axis, the potential of the tip was set to oxygen reduction and after a capacitive current peak the upper curve shows a steady current decrease (region “A”) caused by the diffusion of oxygen away from the tip region. This curve was measured without the reduction of oxygen at the sample. At a time of 6 s the potential of the Pt foil sample was set to oxygen reduction (region “B”). The steep decrease of the lower current curve was caused by the immediate decrease of the oxygen concentration close to the tip. After switching off the reduction potential at the sample and returning it to its former value at a time of 8.5 s the concentration of oxygen rose again due to back diffusion from the surrounding solution, since the oxygen concentration at the platinum foil was reduced

significantly. The difference current between the upper and lower curve is attributed to the reduction of oxygen at the sample and can be used as the measuring signal.

## 5. Project Timeline

Table 4. Timetable represents the PhD schedule and duration of each task.

 Finished Activities  Remaining Activities

Time Task	F09	S10	Su10	F10	S11	Su11	F11	S12	Su12	F12
Literature review										
Surface Roughness measurement										
Mechanical Characterization										
Electrical characterization										
Chemical characterization										
Effect of carbon loading										
In-situ cAFM studies										
Defense										

## 6. Contribution to the Scientific Knowledge

Successful accomplishments of this project will yield knowledge of degradation mechanism as well as to identify measures to improve fuel cell lifetime and reliability. The surface roughness results will provide key insights in understanding the effect of GDL and CL surface characteristics on mass transport and contact resistance losses. Nanoindentation AFM can help to determine elastic modulus of CL under various conditions. Conductive AFM can be a useful technique to study current distribution and estimate conductive areas in CL from beginning to end of life cycle. In-situ cAFM using electrochemical cell will be a novel technique to correlate the structure of CL with local reactivity.

## References

<sup>i</sup> T. Thampan, S. Malhotra, J. Zhang, R. Datta, PEM Fuel Cell as a Membrane Reactor, Catalysis Today, 2001, 67, 15-32.

- 
- <sup>ii</sup> A. Tonkovich, J. Zilka, M. Lamont, Y. Yang, R. Wegeng, Microchannel Reactors for Fuel Cell Processing Applications I. Water Gas Shift Reactor, Chemical Engineering Science, 1999, 54, 2947-2951
- <sup>iii</sup> M. Wilson and S. Gottesfeld, High Performance Catalyzed Membrane of Ultra Low Pt Loadings for Polymer Electrolyte Fuel cells, Journal of Electrochemical Society, 1992, 139, 28-30.
- <sup>iv</sup> V. Paganin, E. Ticlanelli, E. Gonzalez, Development and Electrochemical Studies of Gas diffusion electrodes for Polymer Electrolyte Fuel cell, Journal of Electrochemical Society, 26, 1993, 297-304
- <sup>v</sup> C. Marr, X. Li, Composition and Performance Modeling of Catalyst Layer in a proton Exchange Fuel Cell, Journal of Power Source, 77, 1999, 17-27.
- <sup>vi</sup> H. Gasteiger, S. Kocha, B. Sompalli and F. Wagner, Activity Benchmarks and Requirements for Pt, Pt-alloy, and Non-Pt Oxygen Reduction Catalysts for PEMFCs, Applied Catalyst B, 2005, 56, 9–35.
- <sup>vii</sup> P. Ferreira, O. Y. Shao, D. Morgan, R. Makharia, S. Kocha, Instability of Pt/C Electrocatalysts in Proton Exchange Membrane Fuel Cells. Journal of Electrochemical Society, 152, 2005, A2256–71.
- <sup>viii</sup> K. Yasuda, A. Taniguchi, T. Akita, T. Toroi, Z. Siroma, Characteristics of a Platinum Black Catalyst Layer with Regard to Platinum Dissolution Phenomena in a Membrane Electrode Assembly, Journal of Electrochemical Society, 153, 2006, 599–603.
- <sup>ix</sup> J. Xie, D. Wood III, K. More, P. Atanassov, R. Borup, Microstructural Changes of Membrane Electrode Assemblies During PEFC Durability Testing at High Humidity Conditions, Journal of Electrochemical Society, 152, 2005, A1011–1020.
- <sup>x</sup> M. Watanabe, K. Tsurumi, T. Mizukami, T. Nakamura, P. Stonehart. Activity and Stability of Ordered and Disordered Co-Pt Alloys for Phosphoric Acid Fuel Cells, Journal of Electrochemical Society, 141, 1994, 2659–68.
- <sup>xi</sup> E. Guilminot, A. Corcella, F. Charlot, F. Maillard, M. Chatenet, Detection of Pt<sup>z+</sup> Ions and Pt Nanoparticles Inside the Membrane of a Used PEMFC, Journal of Electrochemical Society, 154, 2007, B96–B105.
- <sup>xii</sup> K. More, R. Borup, K. Reeves, Identifying Contributing Degradation Phenomena in PEM Fuel Cell Membrane Electrode Assemblies via Electron Microscopy, ECS Transaction, 3, 2006, 717–733
- <sup>xiii</sup> R. Dingreville, J. Qu and M. Cherkaoui, Surface Free Energy and its Effect on the Elastic Behavior of Nano-Sized Particles, Wires and Films, Journal of Mechanics Physics Solids, 53, 2005, 1827–1854.
- <sup>xiv</sup> A. Virkar, Y. Zhou, Mechanism of Catalyst Degradation in Proton Exchange Membrane Fuel Cells, Journal of Electrochemical Society, 154, 2007, B540–B547.
- <sup>xv</sup> X. Wang, R. Kumar, D. Myers, Effect of Voltage on Platinum Dissolution, Relevance to Polymer Electrolyte Fuel Cells, Electrochemical and Solid-State Letters, 2006, 9, A225-A227.
- <sup>xvi</sup> R. Borup, J. Davey, F. Garzon, D. Wood, M. Inbody, PEM Fuel Cell Electrocatalyst Durability Measurements, Journal of Power Sources, 2006, 163, 76-81.
- <sup>xvii</sup> K. Mayrhofer, J. Meier, S. Ashton, G. Wiberg, F. Kraus, M. Hanzlik, M. Arenz, Fuel Cell Catalyst Degradation on the Nanoscale, Electrochemical Communication, 10 2008, 1144–1147.

- 
- <sup>xviii</sup> Z. Luo, D. Li, H. Tang, M. Pan, R. Ruan, Degradation Behavior of Membrane-Electrode Assembly Materials in 10-cell PEMFC Stack, *International Journal of Hydrogen Energy*, 31, 2006, 1831-1837.
- <sup>xix</sup> S. Mitsushima, S. Kawahara, K. Ota, N. Kamiya, Consumption Rate of Pt Under Potential Cycling, *Journal of Electrochemical Society*, 154, 2007, B153-B158.
- <sup>xx</sup> S.C. Ball, S.L. Hudson, J.H. Leung, A.E. Russell, D. Thompsett and B.R.C. Theobald, Mechanisms of activity loss in PtCo alloy systems *ECS Trans.* 11 (2007), pp. 1247-1257.
- <sup>xxi</sup> J. Wu, X. Yuan, J. Martin, H. Wang, J. Zhang, J. Shen, S. Wu, W. Merida, A Review of PEM Fuel Cell Durability: Degradation Mechanisms and Mitigation Strategies, *Journal of Power Sources* 184, 2008, 104-119.
- <sup>xxii</sup> Y. Shao, G. Yin, Y. Gao, Understanding and Approaches for the Durability Issues of Pt-Based Catalysts for PEM Fuel Cell, *Journal of Power Sources* 2007, 171, 558-566.
- <sup>xxiii</sup> E. Guilminot, A. Corcella, M. Chatenet, F. Maillard, F. Charlot, G. Berthomé, C. Iojoiu, J. Sanchez, E. Rossinot, E. Clauded, Membrane and Active Layer Degradation upon PEMFC Steady State Operation, *Journal of Electrochemical Society*, 154, 2007, B1106-B1114.
- <sup>xxiv</sup> T. Akita, A. Taniguchi, J. Maekawa, Z. Siroma, K. Tanaka, M. Kohyama, K. Yasuda, Analytical TEM Study of Pt Particle Deposition in the Proton Exchange Membrane of a Membrane Electrode Assembly, *Journal of Power Sources*, 159, (2006), 461-467.
- <sup>xxv</sup> A. Aricò, A. Stassi, E. Modica, R. Ornelas, I. Gatto, E. Passalacqua, V. Antonucci, Evaluation of High Temperature Degradation of Pt/C Catalysts in PEM Fuel Cells, *ECS Transaction*, 3, (2006), 765-774.
- <sup>xxvi</sup> T. Yoda, H. Uchida, M. Watanabe, Effects of Operating Potential and Temperature on Degradation of Electrocatalyst Layer for PEFCs, *Electrochimical Acta*, 52, 2007, 5997-6005.
- <sup>xxvii</sup> Chen, M. Waje, W. Li, Y. Yan, Supportless Pt and Pt-Pd Nanotubes with High Durability and Activity Towards Oxygen Reduction Reaction for PEMFCs, *ECS Transaction*, 11, 2007, 1301-1311.
- <sup>xxviii</sup> Z. Siroma, K. Ishii, K. Yasuda, M. Inaba, A. Tasaka, Stability of Platinum Particles on a Carbon Substrate Investigated by Atomic Force Microscopy and Scanning Electron Microscopy, *Journal of Power Sources*, 171, 2007, 524-529.
- <sup>xxix</sup> D. Bussian, J. O'Dea, H. Metiu, S. Buratto, Nanoscale Current Imaging of the Conducting Channels in Proton Exchange Membrane Fuel Cells, *Nano Letters*, 7, 2007, 227-232.
- <sup>xxx</sup> F. Garzon, S. Lau, J. Davey, R.L. Borup, *ECS Transaction*, 11, 2007, 1139-1150.
- <sup>xxxi</sup> S. Lau, W. Chiu, F. Garzon, H. Chang, A. Tkachuk, M. Feser, W. Yun, Non Invasive, Multiscale 3D X-Ray Characterization of Porous Functional Composites and Membranes, *Journal of Physics Conference Series*, 152, 2009.
- <sup>xxxii</sup> Y. Patil, W. Jarrett and K. Mauritz, Deterioration of Mechanical Properties: A Cause for Fuel Cell Membrane Failure, *Journal of Membrane Science*, 356, 2010, 7-13.
- <sup>xxxiii</sup> E. Aleksandrova, R. Hiesgen, D. Eberhard, A. Friedrich, Proton Conductivity Study of a Fuel Cell Membrane With Nanoscale Resolution, *Journal of Chemical Physics and Physical Chemistry*, 8, 2007, 519-522.
- <sup>xxxiv</sup> R. Hiesgen, E. Aleksandrova, D. Eberhard, A. Friedrich, High Resolution of Ion Conductivity of Nafion Membrane with Electrochemical Atomic Force Microscopy

- <sup>xxxv</sup> X. Cheng, L. Zhang, L. Chen, Y. Zhang and Q. Fan, In-Situ Raman Spectroscopy on PtRu/C in PEMFC, ECS Transaction, 19, 2009, 1-8
- <sup>xxxvi</sup> H. Yamada, D. Shimoda, K. Matsuzawa, A. Tasaka, M. Inaba, Stability of Pt-Ru/C Catalysts: Effect of Ru Content, ECS Transaction, 11, 2007, 325–334.
- <sup>xxxvii</sup> Y. Shao, R. Kou, J. Wang, V. Viswanathan, J. Kwak, J. Liu, Y. Wang, Y. Lin, The Influence of the Electrochemical Stressing (Potential Step and Potential Static Holding) on the Degradation of Polymer Electrolyte Membrane Fuel Cell Electrocatalysts, Journal of Power Sources, 185, 2008, 280–286.
- <sup>xxxviii</sup> W. Bi, T.F. Fuller, Temperature Effects on PEM Fuel Cells Pt/C Catalyst Degradation, Journal of Electrochemical Society, 155, 2008, B215–B221.
- <sup>xxxix</sup> B. Avasarala and P. Halder, Effect of Surface Roughness of Composite Bipolar Plates on the Contact Resistance of a Proton Exchange Membrane Fuel Cell, Journal of Power Source, 188, 2009, 225-229.
- <sup>xl</sup> A. Kraytsberg, M. Auinat, Y. Ein-Eli, Reduced Contact Resistance of PEM Fuel Cell's Bipolar Plates via Surface Texturing, Journal of Power Source, 164, 2007, 697-703.
- <sup>xli</sup> V. Mishra, F. Yang, R. Pitchumani, Measurement and Prediction of Electrical Contact Resistance Between Gas Diffusion Layers and Bipolar Plate for Applications to PEM Fuel Cells, Journal of Fuel Cell and Technology, 1, 2004, 2-9.
- <sup>xlii</sup> Y. Zhou, G. Lin, A.J. Shih, S.J. Hu, A Micro-Scale Model for Predicting Contact Resistance Between Bipolar Plate and Gas Diffusion Layer in PEM Fuel Cells, Journal of Power Source, 163, 2007, 777-783.
- <sup>xliii</sup> L. Zhang, Y. Liu, H. Song, S. Wang, Y. Zhou and S.J. Hu, S.J. Hu, Estimation of contact resistance in proton exchange membrane fuel cells, Journal of Power Source, 162, 2006, 1165-1171.
- <sup>xliv</sup> Z. Wu, S. Wang, L. Zhang, S.J. Hu, An Analytical Model and Parametric Study of Electrical Contact Resistance in Proton Exchange Membrane Fuel Cells, Journal of Power Source, 189, 2009, 1066-1073.
- <sup>xlvi</sup> R. Makharia, M.F. Mathias, D.R. Baker, Measurement of Catalyst Layer Electrolyte Resistance in PEFCs Using Electrochemical Impedance Spectroscopy, Journal of Electrochemical Society, 152, 2005, A970-A975.
- <sup>xlvii</sup> J. Kleemann, F. Finsterwalder, W. Tillmetz, Characterization of Mechanical behavior and Coupled Electrical Properties of Polymer Electrolyte Membrane Fuel Cell Gas Diffusion Layers, Journal of Power Source, 192, 2009, 92-102.
- <sup>xlviii</sup> I. Taymaz, M. benli, Numerical Study of Assembly Pressure Effect on the performance of proton Exchange Membrane Fuel Cell. Energy, 35, 2010, 2134-2140.
- <sup>xlix</sup> X. Wang, H. Zhang, J. Zhang, H. Xu, Z. Tian, J. Chen, H. Zhong, Y. Liang and B. Yi, Micro-porous Layer with Composite Carbon Black for PEM Fuel Cells, Electrochimica Acta, 51, 2006, 4909-4915.
- <sup>l</sup> J. Zhang, G. Yin, Z. Wang, Y. Shao, Effects of MEA Preparation on the Performance of a Direct Methanol Fuel Cell, Journal of Power Source, 160, 2006, 135-140.
- <sup>li</sup> F. Hizir, S. Ural, E. Kumbur, Characterization of Interfacial Morphology in Polymer Electrolyte Fuel Cells: Microporous Layer and Catalyst Layer Surfaces, Journal of Power Source, 195, 2010, 3463-3471.
- <sup>li</sup> S. Kundu, M.W. Fowler, L.C. Simon, S. Grot, Morphological Features (defects) in Fuel Cell Membrane Electrode Assemblies, Journal of Power Source, 157, 2006, 650-656.

- 
- <sup>lii</sup> J. Xie, I.D.L. Wood, K.L. More, P. Atanassov, R.L. Borup, Microstructural Changes of Membrane Electrode Assemblies during PEFC Durability Testing at High Humidity Conditions, *Journal of Electrochemical Society*, 152, 2005, A1011 - A1020.
- <sup>liii</sup> R. McDonald, C. Mittelsteadt and E. Thompson, Effects of Deep Temperature Cycling on Nafion® 112 Membranes and Membrane Electrode Assemblies, *Fuel Cell*, 4, 2004, 208-213.
- <sup>liv</sup> A. Kusoglu, A. Karlsson, M. Santare, S. Cleghorn, W. Johnson, Mechanical Response of Fuel Cell Membranes Subjected to a Hygro-Thermal Cycle, *Journal of Power Source*, 161, 2006, 987-996.
- <sup>lv</sup> Y. Tang, M. Santare, A. Karlsson, S. Cleghorn, W. Johnson, Stresses in Proton Exchange Membranes Due to Hygro-Thermal Loading, *Journal of Fuel Cell Science Technology*, 3, 2006, 119-125.
- <sup>lvi</sup> S. Ahna, S. Shinb, H. Hab, S. Hongb, Y. Leea, T. Limc and I. Ohb, Performance and lifetime analysis of the kW-class PEMFC stack, *Journal of Power Source*, 106, 2002, 295-303.
- <sup>lvii</sup> G. Feng, W. Nix, Y. Yoon, C. Lee, A study of the mechanical properties of nanowires using nanoindentation, *Journal of Applied Physics*, 99, 2006, 45-65.
- <sup>lviii</sup> X. Li, H. Gao, C. Murphy, K. Caswell, Nanoindentation of Silver Nanowires, *Nano Letters*, 3, 2003, 1495- 1498.
- <sup>lix</sup> E. Tan and C. Lim, Nanoindentation Study of Nanofibers, *Applied Physics Letters*, 87, 2005, 1023-1026.
- <sup>lx</sup> S. Logothetidis, S. Kassavetis, C. Charitidis, Y. Panayiotatos and A. Laskarakis, Nanoindentation studies of multilayer amorphous carbon films, *Carbon*, 42, 2004, 1133-1136.
- <sup>lxi</sup> M. Lucas, W. Mai, R. Yang, Z. Wang, E. Riedo, Aspect Ratio Dependence of the Elastic Properties of ZnO Nanobelts, *Nano Letters*, 2007, 7, 1314-1317.
- <sup>lxii</sup> M. Oyen, Nanoindentation Hardness of Mineralized Tissues, *Journal of Biomechanics*, 39, 2006, 2699-2702.
- <sup>lxiii</sup> D. Ebenstien and L. Pruitt, Nanoindentation of Biological Materials, *Nano Today*, 1, 2006, 26-33.
- <sup>lxiv</sup> X. Li and B. Bhushan, Development of continuous stiffness measurement technique for composite magnetic tapes, *Scripta Materialia*, 42, 2000, 929-935.
- <sup>lxv</sup> H. Hertz, Über die Berührung fester elastischer Körper, *J. Reine und Angewandte Mathematik*. 92, 1882, 156.
- <sup>lxvi</sup> K. Pooresh, C. Cho, G. Lee and Y. Tak, , Gradation of Mechanical Properties in Gas Diffusion Electrode. Part 1: Influence of Nano-scale Heterogeneity in Catalyst layer on Interfacial Strength Between Catalyst Layer and Membrane, *Journal of Power Source*, 195, 2010, 2709.
- <sup>lxvii</sup> K. Poornesh, C. Cho, Poroelastic PEM Fuel Cell Catalyst Layer and Its Implication in Predicting the Effect of Mechanical Load on Flow and Transport Properties, *International Journal of Hydrogen Energy*, 36, 2011, 3623.
- <sup>lxviii</sup> D. A. Stevens, M. T. Hicks, G. M. Haugen, J. R. Dahn, Ex Situ and In Situ Stability Studies of PEMFC Catalysts *Journal of The Electrochemical Society*, 152, A2309

- 
- <sup>lxix</sup> Coloma, F.; Sepulveda-Escribano, A.; Fierro, J. L. G.; Rodriguez- Reinoso, F. Preparation of Platinum Supported on Pregraphitized Carbon Blacks, *Langmuir*, 10, 1994, 750.
- <sup>lxx</sup> X. Cheng, L. Zhang, L. Chen, Y. Zhang and Q. Fan, In-Situ Raman Spectroscopy on PtRu/C in PEMFC, *ECS Transaction*, 19, 2009, 1-8
- <sup>lxxi</sup> X. Cheng, L. Chen, C. Peng, Y. Zhang, Q. Fan, Catalyst Microstructure Examination of PEMFC Membrane Electrode Assemblies vs. Time, *Journal of Electrochemical Society*, 151, 2004, A48-A52.
- <sup>lxxii</sup> A. Patterson, The Scherrer Formula for X-Ray Particle Size Determination, *Physics Review*, 56, 1939, 1978-1982.
- <sup>lxxiii</sup> F. Meier, S. Denz, A. Weller, G. Eigenberger, Analysis of Direct Methanol Fuel Cell Performance via FTIR Spectroscopy of Cathode Exhaust, *Fuel Cells*, 3, 2003, 161-169.
- <sup>lxxiv</sup> Q. Fan, C. Pu, E. Smotkin, In-Situ FTIR-diffuse reflection study of Methanol Oxidation Mechanisms of Fuel Cell Anodes, *Energy Conversion Engineering*, 6, 1996, 1112-1116.
- <sup>lxxv</sup> A. Arico, V. Baglio, A. Blasi, V. Atanucci, FTIR Spectroscopic Investigation of Inorganic Fillers for Composite DMFC Membranes, *Electrochemistry Communications*, 5, 2003, 862-866.
- <sup>lxxvi</sup> J. Munk, A. Christensen, A. Hamnett, W. Skou, The Electrochemical Oxidation of Methanol on Platinum and Platinum + Ruthenium Particulate Electrodes Studied by In-situ FTIR Spectroscopy and Electrochemical Mass Spectrometry, *Journal of Electroanalytical Chemistry*, 401, 1996, 215-22.
- <sup>lxxvii</sup> V. Paganin, E. Ticianelli, E. Gonzalez, Development and Electrochemical Studies of Gas Diffusion Electrodes for Polymer Electrolyte Fuel Cells, *Journal of Applied Electrochemistry*, 26, 1996, 297-304.
- <sup>lxxviii</sup> L. Jordan, A. Shukla, T. Behring, Diffusion Layer Parameters Influencing Optimal Fuel Cell Performance. *Journal of Power Sources*, 86, 2000, 250-254
- <sup>lxxix</sup> J. Song, S. Cha, W. Lee, Optimal composition of polymer electrolyte fuel cell electrodes determined by the AC impedance method, *Journal of Power Sources*, 94, 2011, 78-84
- <sup>lxxx</sup> M. Uchida, Y. Fukoka, A. Ohta, Improved Preparation Process of Very-Low-Platinum-Loading Electrodes for Polymer Electrolyte Fuel Cells, *Journal of Electrochemical Society*, 145, 1998, 3708-3713.
- <sup>lxxxi</sup> R. Hiesgen, D. Eberhardt, E. Aleksandrova, K. A. Friedrich, Investigation of Structure and ORR Reactivity of Fuel Cell Catalysts by in-situ STM, *Journal of Electrochemical Society*, 37, 2007, 1495-1502.